

Research Article

A New Coupled Awareness-Epidemic Spreading Model with Neighbor Behavior on Multiplex Networks

Chao Zuo, Anjing Wang, Fenping Zhu, Zeyang Meng, and Xueke Zhao 

School of Management Engineering and E-Commerce, Zhejiang Gongshang University, Hangzhou 310018, China

Correspondence should be addressed to Xueke Zhao; zhaoxueke111@gmail.com

Received 11 December 2020; Revised 19 February 2021; Accepted 26 February 2021; Published 18 March 2021

Academic Editor: xiaoke xu

Copyright © 2021 Chao Zuo et al. This is an open access article distributed under the Creative Commons Attribution License, which permits unrestricted use, distribution, and reproduction in any medium, provided the original work is properly cited.

In this paper, we propose a nonlinear coupled model to study the two interacting processes of awareness diffusion and epidemic spreading on the same individual who is affected by different neighbor behavior status on multiplex networks. We achieve this topology scenario by two kinds of factors, one is the perception factor that can change interplay between different layers of networks and the other is the neighbors' behavior status that can change the infection rate in each layer. According to the microscopic Markov chain approach (MMCA), we analyze the dynamical evolution of the system and derive the theoretical epidemic threshold on uncorrelated heterogeneous networks, and then, we validate the analysis by numerical simulation and discuss the final size of awareness diffusion and epidemic spreading on a scale-free network. With the outbreak of COVID-19, the spread of epidemic in China prompted drastic measures for transmission containment. We examine the effects of these interventions based on modeling of the awareness-epidemic and the COVID-19 epidemic case. The results further demonstrate that the epidemic spreading can be affected by the effective transmission rate of the awareness and neighbors' behavior status.

1. Introduction

The outbreak of COVID-19 can involve the diffusion of information about the epidemic, including the officially released authoritative information, rumors, and fears [1–3]. In reality, awareness diffusion can stimulate individuals to take spontaneous behavioral responses such as wearing masks or staying at home to reduce the frequency of face-to-face contact [4, 5]. Therefore, the epidemic-spreading dynamics in complex networks has attracted increasing attention in many disciplines [6, 7]. However, the exact impact they can have on the epidemic dynamics is difficult to quantify, so mathematical modelling is used to test hypotheses and identify pivotal parameters in the interplay between awareness diffusion and epidemic spreading [8–11]. For example, Granell et al. constructed a UAU-SIS (unaware-aware-unaware/susceptible-infected-susceptible) model to study the interaction between epidemics spreading and awareness diffusion on multiplex networks [12]. Funk et al. researched the coevolution of information and epidemic on public and found that the spread of

positively oriented information about the epidemic can suppress the epidemic [13]. Wang et al. utilized real data to investigate the coevolution mechanisms between information and disease spreading, and the empirical analysis showed that there is an asymmetric interaction between information and disease spreading [14]. Moreover, Wang et al. further found that the awareness inhibits the epidemic spreading, whereas the epidemic spreading facilitates the awareness diffusion [15]. Zhu et al. thought that an epidemic might spread among multicommunities, so they modeled each community as a multiplex network that included both a virtual awareness layer and a physical layer [16]. They further presented a coupled UAU-SIRD model, which consisted of a virtual layer sustaining unaware-aware-unaware dynamics and a physical layer supporting the susceptible-infected-recovered-dead process, to investigate the spreading property of epidemics and the relationships between the focused variables and parameters of the epidemic. The result indicated that the incorporation of virtual layers would reduce the range of affected individuals [17]. Kabir and Tanimoto established

a two-layer SIR-UA (susceptible-infected-recovered/unaware-aware) epidemic transmission model that comprehensively considered the influence of individual behavior and awareness diffusion on epidemic spreading on heterogeneous networks [18]. Shang studied the effects of global, local, and contact awareness on a discrete-time SIS epidemic dynamics and used the stability theory of matrix difference equation to derive the epidemic threshold [19]. They further investigated the impact of the three forms of awareness on epidemic spreading by the mean-field approach with heterogeneous transmission rates, and the numerical simulation results showed that both local and contact awareness can raise the epidemic threshold while global awareness can only decrease the final epidemic size [20].

Though the effects of information-based behavioral responses on the epidemic dynamics have been studied by many documents, most of them assumed that individuals are treated equally when they contact different neighbors. In fact, the deviation among different neighbors has a remarkable influence on the individual infection process due to the complex topological structures of networks. In view of this, there has been an increasing focus on the discussion of neighbor behavior in the interacting processes of awareness diffusion and epidemic spreading [21–25]. For instance, Kan and Zhang assumed that susceptible individuals can not only be informed by aware neighbors in the information network but also by self-awareness induced by the infected neighbors in the contact network. Results indicated that the individuals with more neighbors in the information network have higher awareness acquisition and they are hard to be infected in the contact network [26]. Guo et al. introduced a heterogeneous threshold model to converse that a hub with a large number of neighbors is relatively easy to become infected [6]. Moreover, they proposed a heterogeneous spreading model that considers the degree heterogeneity and k -core measures heterogeneity of individuals with the belief that different individuals facing the same epidemic would exhibit distinct behaviors according to their own experiences and attributes [27]. Zhu et al. generated an adaptive strategy of the susceptible/exposed individual that a susceptible/exposed individual would disconnect with infected neighbors probabilistically and one new connection would be constructed [28]. Chen et al. proposed a resource-epidemic coevolution model to investigate the effects of the heterogeneous distribution of self-awareness and the heterogeneous distribution of node degree on the epidemic dynamics. They found that the heterogeneity of self-awareness distribution suppresses the outbreak of an epidemic and the heterogeneity of degree distribution enhances the epidemic spreading [29]. Pan and Yan proposed a coupled awareness-epidemic spreading model incorporating the heterogeneity of neighbors' responses to disease outbreaks, and the result showed that the heterogeneity of neighbors' responses acts on the epidemic threshold in the higher stage [30].

Some research studies assumed that the diffusion of awareness will reduce the infection rate of individuals [12–16]. Considering that the spread rate of awareness is also affected

by the spread of the epidemic [15], in this work, the awareness perception factor f_1 ($0 \leq f_1 \leq 2$) stands for the influence of awareness diffusion on the spread rate of epidemic, and we also introduce an epidemic perception factor f_2 ($0 \leq f_2 \leq 2$) to express the impact of epidemic spreading on the diffusion rate of awareness. We define $f_1 \leq 1$, $f_2 > 1$ when authoritative information and epidemic interact and rule $f_1 > 1$, $f_2 \leq 1$ when rumors and epidemic interact, as shown in Table 1.

Moreover, Kan and Zhang discussed the effect of infected neighbors on the formation of node self-awareness [26], and some references confirmed that the heterogeneity of degree distribution enhances the epidemic spreading [27, 29]. On this basis, we assume that the health of awareness neighbors (susceptible, infected, and recovered) plays different roles in the formation of node self-awareness and propose the health-impact-awareness status factors ($\Delta\rho_1$, $\Delta\rho_2$, and $\Delta\rho_3$) to distinguish this effect in the awareness layer; the heterogeneity of neighbors degree distribution will affect the individual's epidemic infection rate, and the behavior-impact-epidemic status factor ($1 - e^{(-k_j/\sum k)}$, a positive correlation function of neighbors degree) is established to discriminate the difference in the epidemic layer. Therefore, we propose a multiplex networks model to comprehend the spreading dynamics between epidemic and awareness on the same population with the influence of different neighbor behavior status. We introduce the behavior status to each node in the multiplex networks. On the one hand, people can acquire awareness from aware neighbors with different health-impact-awareness status in layer 1 of fictitious contacts, such as Microblogs, WeChat, or other social media. On the other hand, in layer 2 of physical contacts, the level of epidemic spreading would be influenced by the infected neighbors with different behavior-impact-epidemic status. The MMCA theoretical analysis and numerical simulations results reveal that awareness and behavioral changes could have favorable effects on the epidemic spreading.

The rest of this paper is organized as follows: in Section 2, we introduce the multiplex networks model. Then, we analyze the dynamical processes of the model with the MMCA method and derive the expression of epidemic threshold in Section 3. Next, in Sections 4 and 5, we perform numerical simulations and discuss the Chinese COVID-19 epidemic case to validate theoretical predictions. Finally, we summarize our findings and conclusions in Section 6.

2. Nonlinear Coupled Awareness-Epidemic Model

2.1. Model Descriptions. In this work, we generalize a multiplex networks model to formalize and simplify the spread mechanisms, as illustrated in Figure 1. In layer 1, people share epidemic-prevention awareness through social media, while people get infected in layer 2. Neighbor behavior is simplified as the “health-impact-awareness” status of aware neighbors in layer 1 and the “behavior-impact-epidemic” status of infected neighbors in layer 2. The definitions of key parameters are shown in Table 2. We suppose the multiplex propagation process according to the following regulations:

TABLE 1: Parameter meaning and influence on individual behavior.

Parameter	Model	Individual behavior
$f_1 < 1$	Authoritative information and epidemic	The ability of conscious individuals to prevent virus increases as f_1 decreases
$f_1 > 1$	Rumors and epidemic	The contribution of conscious individuals to virus spread increases as f_1 increases
$f_2 > 1$	Authoritative information and epidemic	The willingness of infected individuals to transmit information increases as f_2 increases
$f_2 < 1$	Rumors and epidemic	The resistance of infected individuals to rumor increases as f_2 decreases

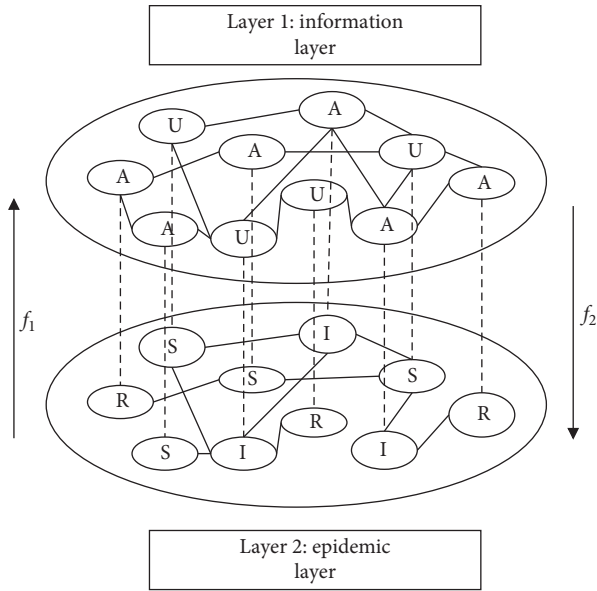


FIGURE 1: UAU-SIR model. Awareness is disseminating in layer 1, and the nodes have two possible states: unaware (U) or aware (A). Epidemic is spreading in layer 2, where the nodes have three possible states: susceptible (S), infected (I), and recovered (R).

- (i) Awareness diffusion in layer 1: the diffusion of awareness satisfies the UAU (unaware-aware-unaware) process. Aware (A) individuals can apply their awareness to decrease the probability of being infected. Unaware (U) individuals do not have any awareness about the epidemic prevention. Unaware individuals can contact with aware neighbors to get awareness with probability λ , while the aware individuals can forget the awareness with probability δ . As we all know, in many cases, individuals who are infected or cured are more aware than those who are far away from the epidemic because once they are exposed to a certain infectious disease (such as SARS or COVID-19), they will be isolated and feel panicked, that is, whether an individual has been physically exposed to the epidemic changes the probability of awareness acquisition. Therefore, we assume that unaware infected (UI) and unaware recovered (UR) individuals know about the epidemic and can increase the probability of being aware with the epidemic perception factor f_2 . Then,

the awareness infection rate can be represented by the susceptible infection rate $\lambda_S = \lambda$ and infected (recovered) infection rate $\lambda_I = f_2 \lambda$ ($\lambda_R = f_2 \lambda$), respectively.

- (ii) Epidemic spreading in layer 2: the spreading of epidemic satisfies the SIR (susceptible-infected-recovered) process. Susceptible individuals get infected with the probability β , while the infected individuals recover with the probability μ . Yet, aware susceptible (AS) individuals can apply the awareness to decrease the probability of being infected with the awareness perception factor f_1 . Then, the epidemic infection rate can be expressed by the unawareness of infection rate $\beta_U = \beta$ and awareness of infection rate $\beta_A = f_1 \beta$, respectively.
- (iii) The health-impact-awareness status of aware neighbors: the direct application of the UAU model in the two-layer network means that the default importance ratio of aware neighbors is AS:AI:AR=1/3:1/3:1/3. We believe that the aware neighbors of different health states play different roles in the process of awareness diffusion and assume that the importance ratio is AS:AI:AR=1/3 + $\Delta\rho_1$:1/3 + $\Delta\rho_2$:1/3 + $\Delta\rho_3$ ($\Delta\rho_1 + \Delta\rho_2 + \Delta\rho_3 = 0$). $\Delta\rho_1$, $\Delta\rho_2$, and $\Delta\rho_3$ are the health-impact-awareness status factors of the model, as shown in Figure 2.
- (iv) The behavior-impact-epidemic status of infected neighbors: the heterogeneity of degree distribution plays a role in the epidemic spreading, and we believe that infected individuals with a large range of daily activities (a large node degree) are more likely to carry and transmit the virus. We use the degree k_j of neighbor j to represent its daily activity range and use $\sum k$ to represent the total degrees of all infected neighbors; as shown in Figure 3, $1 - e^{-(k_j/\sum k)}$ can distinguish the impact of each infected neighbor on epidemic infected probability and also limit the size of this impact (the interval is 0-0.5).

2.2. *Dynamic Model.* According to these presumptions, there are six primary states: US (unawareness susceptibility); UI (unawareness infection); UR (unawareness recovered); AS (awareness susceptibility); AI (awareness infected); and

TABLE 2: The definitions of key parameters.

Parameter	Description
β	Probability of getting infected for susceptible individuals (the basic infection rate)
μ	Probability of recovery
λ	Probability of becoming aware (the basic infection rate)
δ	Probability of becoming unaware
f_1	The awareness perception factor
f_2	The epidemic perception factor
$\Delta\rho_1, \Delta\rho_2, \text{ and } \Delta\rho_3$	The health-impact-awareness status influence of aware neighbors
$(1 - e^{-(k_j/\sum k)})$	The behavior-impact-epidemic status influence of infected neighbors

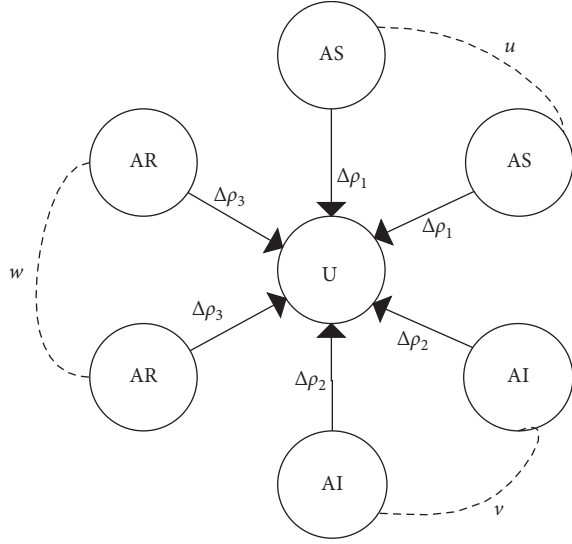


FIGURE 2: Explanation of the health-impact-awareness status of aware neighbors in layer 1. The numbers of AS, AI, and AR are u , v , and w , respectively. Also, the health-impact-awareness factors of the three aware neighbors are $\Delta\rho_1$, $\Delta\rho_2$, and $\Delta\rho_3$, respectively.

AR (awareness recovered). The reaction procedure of the model can be schematically expressed as follows:

- (i) Awareness diffusion $US + AS \xrightarrow{\lambda, 1 + \Delta\rho_1} AS + AS$, $US + AI \xrightarrow{\lambda, 1 + \Delta\rho_2} AS + AI$, $US + AR \xrightarrow{\lambda, 1 + \Delta\rho_3} AS + AR$, $UI + AS \xrightarrow{f_2 * \lambda, 1 + \Delta\rho_1} AI + AS$, $UI + AI \xrightarrow{f_2 * \lambda, 1 + \Delta\rho_2} AI + AI$, $UI + AR \xrightarrow{f_2 * \lambda, 1 + \Delta\rho_3} AI + AR$, $UR + AS \xrightarrow{f_2 * \lambda, 1 + \Delta\rho_1} AR + AS$, $UR + AI \xrightarrow{f_2 * \lambda, 1 + \Delta\rho_2} AR + AI$, $UR + AR \xrightarrow{f_2 * \lambda, 1 + \Delta\rho_3} AR + AR$
- (ii) Epidemic spreading $US + I \xrightarrow{\beta, 1 + (1 - e^{-k_j/\sum k})} AI + I$, $AS + I \xrightarrow{f_1 * \beta, 1 + (1 - e^{-k_j/\sum k})} AI + I$

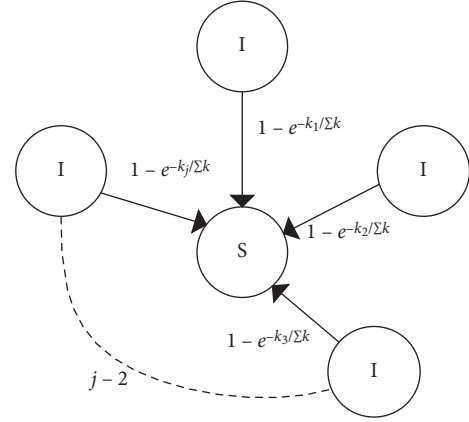


FIGURE 3: Illustration of the behavior-impact-epidemic status of infected neighbors in layer 2. j is the total number of an individual's infected neighbors, and $1 - e^{-(k_j/\sum k)}$ is a positive correlation function of each neighbor's degree.

- (iii) Recoveries $I \xrightarrow{\mu} R$, $A \xrightarrow{\delta} S$

3. Microscopic Markov Chain Approach

We analyze the dynamical processes of the model with the MMCA method [31, 32]. Let x_{ij} and y_{ij} be the adjacency matrices that support the UAU and SIR processes, respectively. The probability of node i in one of the six states at time t is denoted by $P_i^{US}(t)$, $P_i^{UI}(t)$, $P_i^{UR}(t)$, $P_i^{AS}(t)$, $P_i^{AI}(t)$, and $P_i^{AR}(t)$, respectively. Provisions $P_i^{US}(t) + P_i^{UI}(t) + P_i^{UR}(t) + P_i^{AS}(t) + P_i^{AI}(t) + P_i^{AR}(t) = 1$. Under the assumption that the possibilities of becoming aware or infected by any neighbor are independent, we use $r_i^*(t)$, $r_i'(t)$, q_i^{A*} , and q_i^{U*} to represent four basic quantities as follows:

$$\begin{aligned}
 r_i^*(t) &= \Pi_u \left\{ \left[1 - x_{ui} P_u^{AS}(t) \lambda \right]^{(1+\rho_1)} \right\} + \Pi_v \left\{ \left[1 - x_{vi} P_v^{AI}(t) \lambda \right]^{(1+\rho_2)} \right\} + \Pi_w \left\{ \left[1 - x_{wi} P_w^{AR}(t) \lambda \right]^{(1+\rho_3)} \right\}, \\
 r_i'(t) &= \Pi_u \left\{ \left[1 - x_{ui} P_u^{AS}(t) f_2 \lambda \right]^{(1+\rho_1)} \right\} + \Pi_v \left\{ \left[1 - x_{vi} P_v^{AI}(t) f_2 \lambda \right]^{(1+\rho_2)} \right\} + \Pi_w \left\{ \left[1 - x_{wi} P_w^{AR}(t) f_2 \lambda \right]^{(1+\rho_3)} \right\},
 \end{aligned} \tag{1}$$

where $r_i^*(t)$ denotes the probability for susceptible node i not getting aware by any neighbors. $r'_i(t)$ is the probability for infected (recovered) node i not getting aware by any neighbors. x_{ui} means that node i has u neighbors in state P_i^{AS} :

$$\begin{aligned} q_i^{A*} &= \Pi_j [1 - y_{ji} P_j^I(t) f_1 \beta]^{1 + (-k_{j'} \sum k)}, \\ q_i^{U*} &= \Pi_j [1 - y_{ji} P_j^I(t) \beta]^{1 + (-k_{j'} \sum k)}, \end{aligned} \quad (2)$$

where q_i^{A*} (q_i^{U*}) denotes the probability of susceptible aware (unaware) node i not being infected by any neighbors and $y_{ji} = 1$ means that node j is the neighbor of node i at the same layer. We extend Markov's theory to steady state and

assume that $P_i^{AI} + P_i^{UI} = P_i^I = \pi_i \ll 1$. We can obtain the approximations of q_i^{A*} and q_i^{U*} as follows:

$$\begin{aligned} q_i^{A*} &\approx \left(1 - f_1 \beta \sum_j \left(2 - e^{(-k_{j'} \sum k)} \right) y_{ji} \pi_j \right), \\ q_i^{U*} &\approx \left(1 - \beta \sum_j \left(2 - e^{(-k_{j'} \sum k)} \right) y_{ji} \pi_j \right). \end{aligned} \quad (3)$$

The potential state transition process of the UAU-SIR model is shown in Figure 4.

As shown in Figure 4, every time step is divided into six stages, and we can easily get the MMCA equations for node i as follows:

$$\begin{cases} P_i^{US}(t+1) = P_i^{US}(t) r_i^*(t) q_i^{U*}(t) + P_i^{AS}(t) \sigma q_i^{U*}(t), \\ P_i^{UI}(t+1) = P_i^{US}(t) r_i^*(t) [1 - q_i^{U*}(t)] + P_i^{UI}(t) r'_i(t) (1 - \mu) + P_i^{AS}(t) \sigma [1 - q_i^{U*}(t)] + P_i^{AI}(t) \sigma (1 - \mu), \\ P_i^{UR}(t+1) = P_i^{UI}(t) r'_i(t) \mu + P_i^{UR}(t) r'_i(t) + P_i^{AI}(t) \sigma \mu + P_i^{AR}(t) \sigma, \\ P_i^{AS}(t+1) = P_i^{US}(t) (1 - r_i^*(t)) q_i^{A*}(t) + P_i^{AS}(t) (1 - \sigma) q_i^{A*}(t), \\ P_i^{AI}(t+1) = P_i^{US}(t) (1 - r_i^*(t)) [1 - q_i^{A*}(t)] + P_i^{UI}(t) [1 - r'_i(t)] (1 - \mu) + P_i^{AS}(t) (1 - \sigma) [1 - q_i^{A*}(t)] + P_i^{AI}(t) (1 - \mu) (1 - \sigma), \\ P_i^{AR}(t+1) = P_i^{UI}(t) (1 - r'_i(t)) \mu + P_i^{UR}(t) (1 - r'_i(t)) + P_i^{AI}(t) (1 - \sigma) \mu + P_i^{AR}(t) (1 - \sigma). \end{cases} \quad (4)$$

The solution of equation (4) is a set of fixed-point equations that satisfy $P_i^{AI}(t+1) = P_i^{AI}(t) = P_i^{AI}$, and this relationship is also true for the other five types of nodes. We add the second and the fifth equations in equation (4) as follows:

$$\begin{aligned} \mu P_i^I &= P_i^{US}(t) \{ r_i^*(t) [1 - q_i^{U*}(t)] + (1 - r_i^*(t)) [1 - q_i^{A*}(t)] \} \\ &\quad + P_i^{AS}(t) \{ \sigma [1 - q_i^{U*}(t)] + (1 - \sigma) [1 - q_i^{A*}(t)] \}. \end{aligned} \quad (5)$$

Near the threshold, the probability of nodes being infected is very small, i.e., $P_i^{AI} + P_i^{UI} = P_i^I = \pi_i \ll 1$. Taking equation (3) into equation (4) and omitting the $O(\epsilon)$ terms, we get

$$\begin{cases} P_i^{US} = P_i^{US} r_i^*(t) + P_i^{AS}(t) \sigma, \\ P_i^{AS} = P_i^{US} (1 - r_i^*(t)) + P_i^{AS} (1 - \sigma). \end{cases} \quad (6)$$

Substituting (6) into (5), we get

$$\begin{aligned} \mu P_i^I &= \mu \pi_i = P_i^{US} [1 - q_i^{U*}(t)] + P_i^{AS} [1 - q_i^{A*}(t)] \\ &= (P_i^{US} + f_1 P_i^{AS}) \beta \sum_j \left(2 - e^{(-k_{j'} \sum K)} \right) y_{ji} \pi_j, \end{aligned} \quad (7)$$

with $P_i^{AS} \approx P_i^A$, $P_i^{US} \approx 1 - P_i^A$, then, equation (7) can be rewritten as

$$\sum_j \left\{ \left[1 - (1 - f_1) P_i^A \right] \left(2 - e^{(-k_{j'} \sum k)} \right) y_{ji} - \frac{\mu}{\beta} \tau_{ij} \right\} = 0, \quad (8)$$

where τ_{ij} denotes the elements of the identity matrix. We define a new matrix H , where $h_{ij} = [1 - (1 - f_1) P_i^A] (2 - e^{(-k_{j'} \sum k)}) y_{ji}$, to simplify equation (8). The epidemic threshold is equal to the minimum value of β that satisfies equation (8). We can obtain the epidemic threshold by denoting $\Lambda_{\max}(h)$, the maximum eigenvalue of H , and the threshold formula is

$$\beta_c = \frac{\mu}{\Lambda_{\max}(H)}. \quad (9)$$

Equations (8) and (9) show that the epidemic threshold is based on the structure of layer 2 (y_{ji}), the parameter f_1 , and the density of awareness P_i^A . The value of P_i^A is further determined by the structure of layer 1 (x_{ji}), the transmission rate λ , and the recovery rate σ .

4. Results

We discuss the effect of f_1 and f_2 through Model I, on which we introduce the neighbor behavior state, and obtain Model II. The comparison between Model 1 and Model 2 reflects the influence of the neighbor behavior state on the propagation process. We perform extensive Monte Carlo numerical simulations [33, 34] for the model (run 100 times) and obtain the infection density ρ_I and aware density ρ_A at steady state. $\rho_I = (\sum_i \rho_i^I / N) = (\sum_i \rho_i^{AI} / N)$ and $\rho_A = (\sum_i \rho_i^A / N)$, where N represents the number of all individuals in the model. In our simulations, the size of the two-layer network is $N = 1000$, the initial number of nodes $m_0 = 5$, the number of connected edges $m = 3$, and the average degree $\langle k \rangle = 6$. The default value of the parameter is

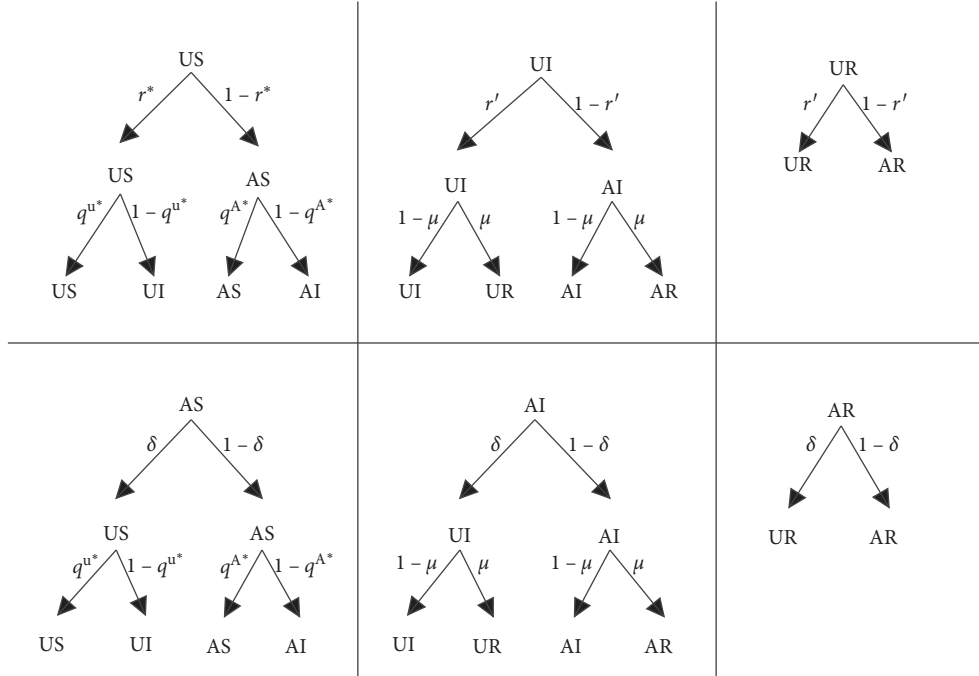
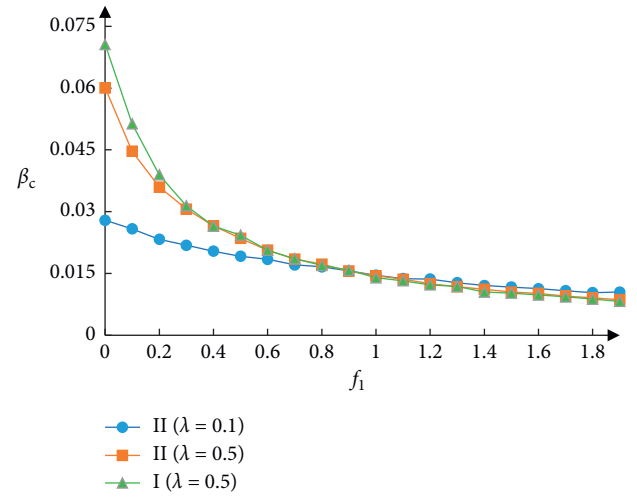


FIGURE 4: Transition probability trees for six possible states.

fixed as $\lambda = 0.5, \sigma = 0.3, \beta = 0.5, \mu = 0.2, f_1 = 1, f_2 = 1, \Delta\rho_1 = 0.067 - 1/3, \Delta\rho_2 = 0.689 - 1/3, \Delta\rho_3 = 0.244 - 1/3$ (the values of $\Delta\rho_1, \Delta\rho_2,$ and $\Delta\rho_3$ in this paper can be set according to actual requirements. We believe that the awareness-spreading intensity of different neighbors is $AI > AR > AS$, and by the summation product method and consistency test, we obtain the importance ratio $AS : AI : AR = 0.067, 0.689, 0.244$).

4.1. Threshold. Figure 5 plots the density of β_c as a decreasing function of f_1 . It is clear that β_c obviously decreases as f_1 ($f_1 \in (0, 1)$) increases and basically remains unchanged as f_1 , ($f_1 \in (1, 2)$) increases. Figure 6 presents that β_c grows as λ increases ($f_1 = 0.2, f_2 = 1.8$) and β_c decreases as λ increases ($f_1 = 1.8, f_2 = 0.2$), which means authoritative information can inhibit the outbreak of the epidemic and rumors will contribute to the spread of the epidemic. At the same time, a smaller information forgetting rate, a greater rumor forgetting rate, and a greater infectious diseases recovery rate can raise the epidemic threshold. Moreover, the curve of Model II is lower than that of Model I with equal parameters in both Figures 5 and 6; measures such as locating and isolating infected neighbors are good ways to prevent an outbreak of the epidemic.

As shown in Figure 7, λ_c is a decreasing function of f_2 . It is clear that λ_c obviously decreases as f_2 ($f_2 \in (0, 1)$) increases and basically remains unchanged as f_2 ($f_2 \in (1, 2)$) increases. Figure 8 suggests that λ_c grows as β increases ($f_1 = 1.8, f_2 = 0.2$) and λ_c decreases as β increases ($f_1 = 0.2, f_2 = 1.8$), which means that the rapid spread of the epidemic can inhibit the outbreak of rumors and promote the dissemination of authoritative information. A smaller information forgetting rate, a greater rumor

FIGURE 5: The influence of f_1 on β_c .

forgetting rate, and a greater infectious disease recovery rate can raise the awareness threshold. Moreover, the curve of Model II is lower than that of Model I with equal parameters in both Figures 7 and 8, publicizing the epidemic information through the infected and cured people will contribute to spreading crisis awareness and preventing the outbreak of the epidemic.

4.2. Infection Scale. The key influencing factors for ρ_I and ρ_A are f_1 and f_2 , respectively. Figure 9 reveals that a larger epidemic cure rate μ helps control the epidemic diffusion scale and a smaller awareness forgetting rate σ contributes to the spread of awareness.

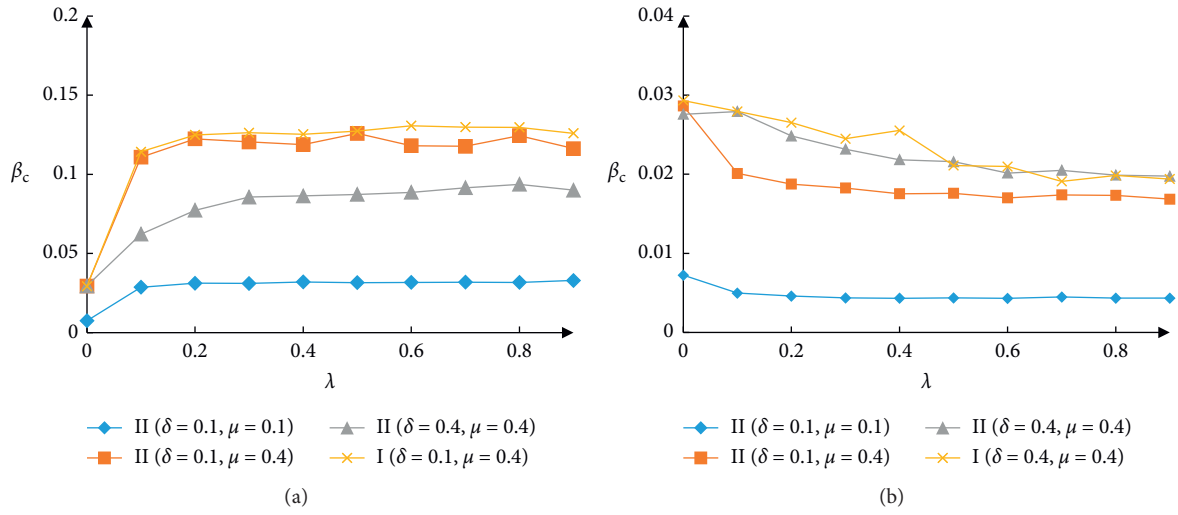


FIGURE 6: The influence of λ on β_c : (a) $f_1 = 0.2, f_2 = 1.8$; (b) $f_1 = 1.8, f_2 = 0.2$.

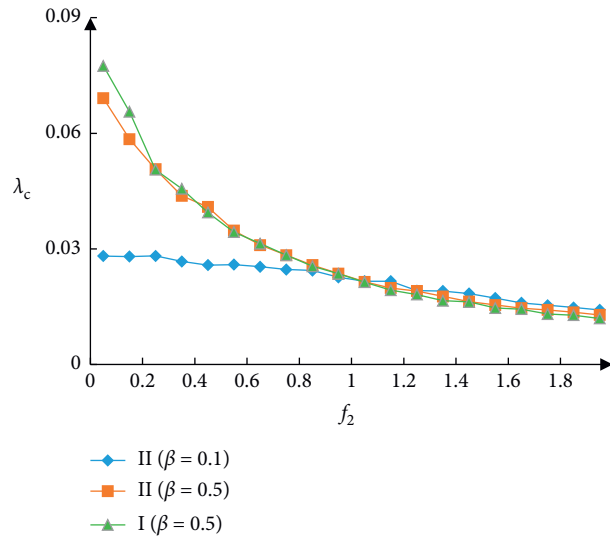


FIGURE 7: The influence of f_2 on λ_c .

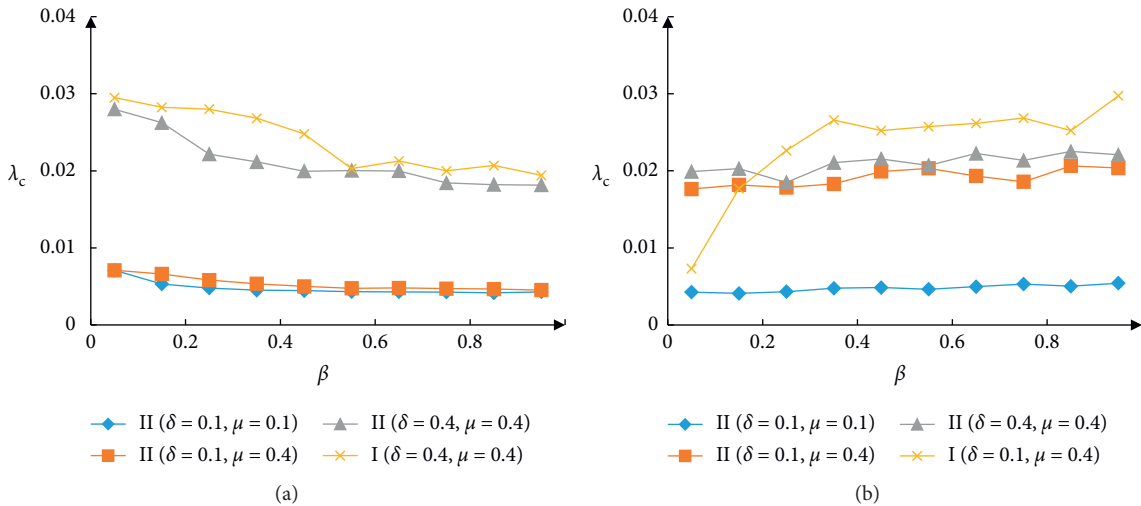


FIGURE 8: The influence of β on λ_c : (a) $f_1 = 0.2, f_2 = 1.8$; (b) $f_1 = 1.8, f_2 = 0.2$.

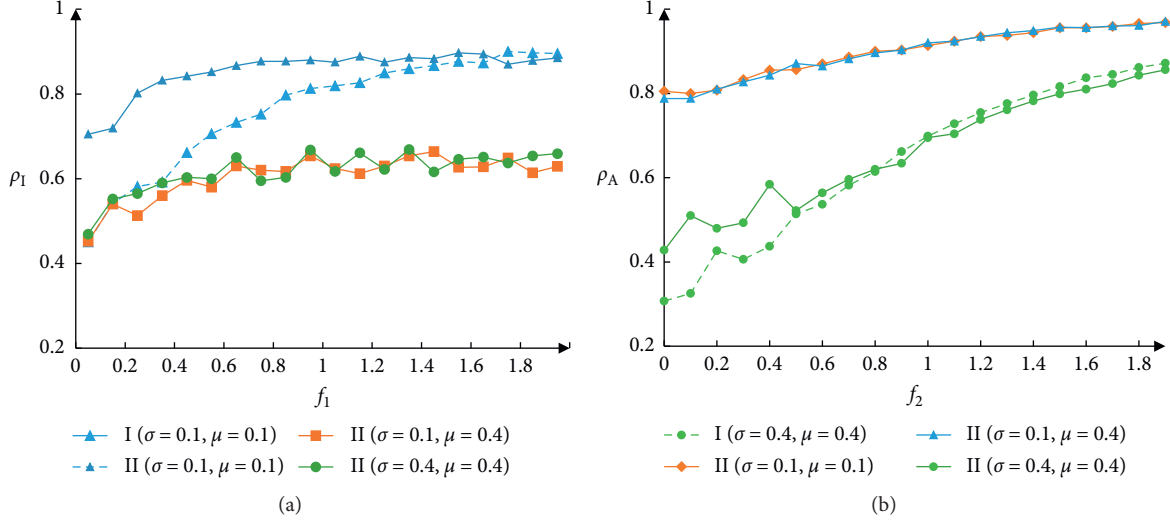


FIGURE 9: Impact of influence factors on the scale of infection.

4.2.1. Authoritative Information and Epidemic Interaction Model ($f_1 < 1, f_2 > 1$). Both ρ_A and ρ_I in Figure 10 show an upward trend with the increase of β , while the curve in Figure 10(a) is less obvious than that in Figure 10(b) because β can only indirectly affect the dissemination of authoritative information. In the meanwhile, a higher prevention degree of the individuals ($f_1 = 0.1$) corresponds to a smaller ρ_I (Figure 10(b)) and a smaller ρ_A (Figure 10(a)). Also, a stronger willingness of the individuals to spread information ($f_2 = 1.8$) led to a larger ρ_A and a smaller ρ_I .

The increase of λ contributes to the spread of awareness (Figure 11(a)) and the reduction of the epidemic scale (Figure 11(b)), which is in line with the actual situation. When the individuals' willingness to disseminate information gets stronger, ($f_2 = 1.8$), the value of ρ_A will be larger and ρ_I will decrease more. A higher prevention degree of the individuals ($f_1 = 0.1$) corresponds to a small ρ_I and a larger ρ_A .

The comparative experimental results of Figures 10 and 11 show that, under the same conditions, the ρ_A obtained by Model II is smaller and ρ_I is larger than that obtained by Model I, which suggests that models ignoring neighbors' behavior status would underestimate the epidemic scale and limit the formulation of epidemic control strategies.

4.2.2. Rumor and Epidemic Interaction Model ($f_1 > 1, f_2 < 1$). A larger β means a greater risk of individual infection, and it will lead to a larger ρ_I . However, rumors are not beneficial to epidemic control, and individuals would resist the spread of rumors; then, the curve of ρ_A would drop. As shown in Figure 12, a smaller f_2 ($f_2 = 0.1$) will lead to a smaller ρ_A , and a larger f_1 , ($f_1 = 1.8$) will cause a larger ρ_I .

A larger λ means that individuals are more likely to have rumor awareness, which will lead to a larger ρ_A . However, individuals in the epidemic layer affected by rumors will take improper behaviors to accelerate the spread of the epidemic, and the ρ_I curve will rise, as illustrated in Figure 13.

Furthermore, the more resistant an individual is to the rumor ($f_2 = 0.1$), the more difficult it is for the rumor to spread in the population, and ρ_A and ρ_I will be smaller; the greater an individual's contribution to epidemic transmission ($f_1 = 1.8$), the easier it is for the epidemic to spread, and ρ_A and ρ_I will be larger.

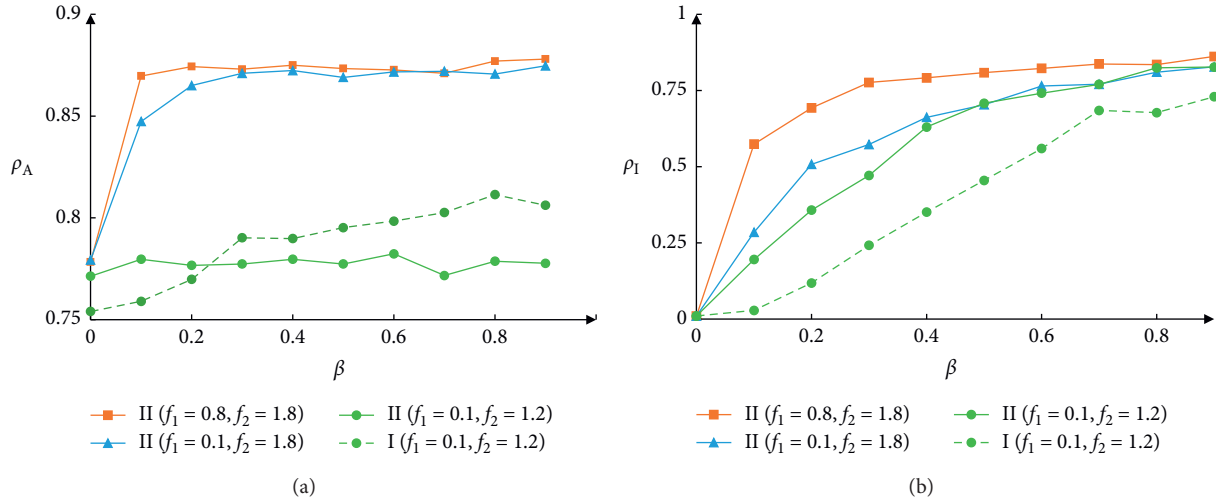
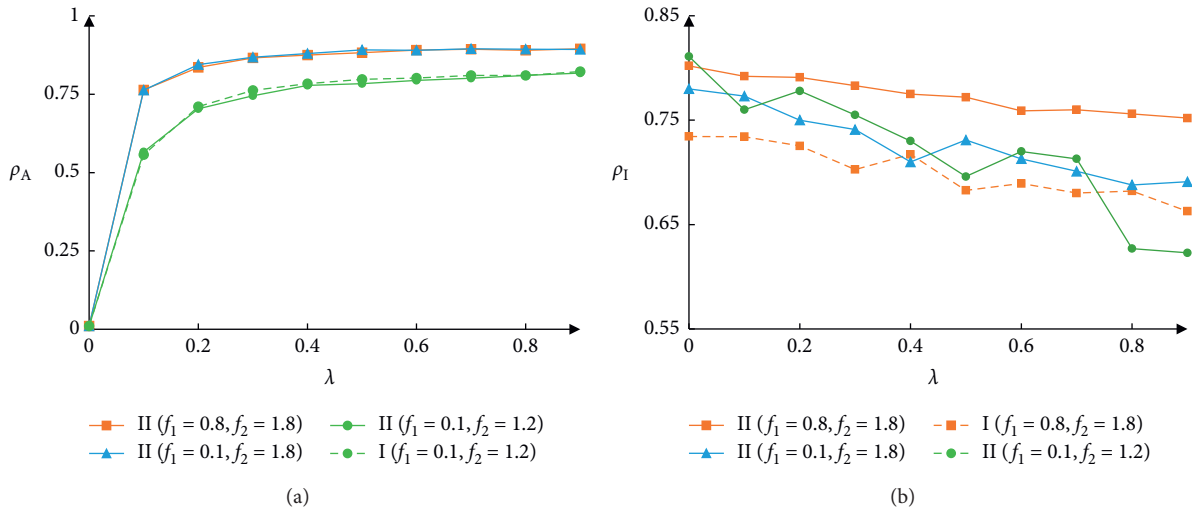
Figures 12 and 13 show that when the spread of the epidemic is accompanied by rumors, ρ_A obtained by Model II is larger than Model I, and the obtained ρ_I is smaller than Model I, which suggests that models ignoring neighbors' behavior status would overvalue the epidemic scale and influence the formulation of epidemic control strategies. As a result, it is necessary and reasonable to consider the influence of neighbors' behavior status when we establish an interactive propagation model.

5. Epidemic Analysis of COVID-19 in China

Four stages of strict measures for transmission containment were prompted during the early spread of COVID-19 in China, which reflects the change in public awareness. Each awareness stage plays discrepant roles in epidemic control and public response behaviors. We hypothesized that the awareness impact factor f_1 is negatively correlated with the importance of epidemic control measures and observe the assumed value of f_1 as shown in Table 3 [35].

Model I and Model II simulate the density of infected individuals as a function of t for different values of f_1 . It is clear that the large value of f_1 can increase the density of infected individuals, see Figure 14(a), and the neighbor behavior status can narrow the gap between the effects of different f_1 on the infection scale, see Figure 14(b). Therefore, the government can actively release positive information to enhance public awareness and restrict the behavior of infected neighbors for the purpose of controlling the spread of the epidemic during the COVID-19 epidemic.

Figure 15 is the daily new data released by the Publicity Department of the National Health Commission except for

FIGURE 10: The influence of β on ρ_A and ρ_I .FIGURE 11: The influence of λ on ρ_A and ρ_I .

Hubei Province, and Figure 16 is the data fitting curve of infected individuals (except Hubei Province). Figures 15 and 16 indicate that the number of infected individuals is gradually decreasing since January 29 with the strengthening of prevention and control measure [36].

Figure 17 shows the cumulative number of confirmed cases in Hubei Province from January to April. Since February 16, the cumulative number of confirmed cases has been close to 0, indicating that the epidemic has been under control. As we all know, public awareness is affected by the spread of the epidemic, and if the epidemic is effectively controlled, public awareness will become weaker. Public awareness is difficult to quantify, but we found such a phenomenon: the online big data information demonstrates that the amount of comprehensive information has risen rapidly since January 20, 2020, and reached the peak on February 15, and the peak time coincides with the epidemic

control time (Feb 16), as shown in Figure 17, which reflect the influence of epidemic spreading on the diffusion of awareness.

As shown in Table 4, the Hubei Provincial Government adjusts information report management at different stages of the epidemic. Each epidemic stage plays discrepant roles in public awareness diffusion. We hypothesized that the epidemic impact factor f_2 is positively correlated with the importance of information report management and observe the assumed value of f_2 .

Model I and Model II simulate the density of aware individuals as a function of t for different values of f_2 . It is clear that the large value of f_1 can increase the density of aware individuals, see Figure 18(a), and neighbor behavior status can expand the gap between the effects of different f_2 on the awareness scale, see Figure 18(b). Therefore, the measures taken by the government to publicize the epidemic

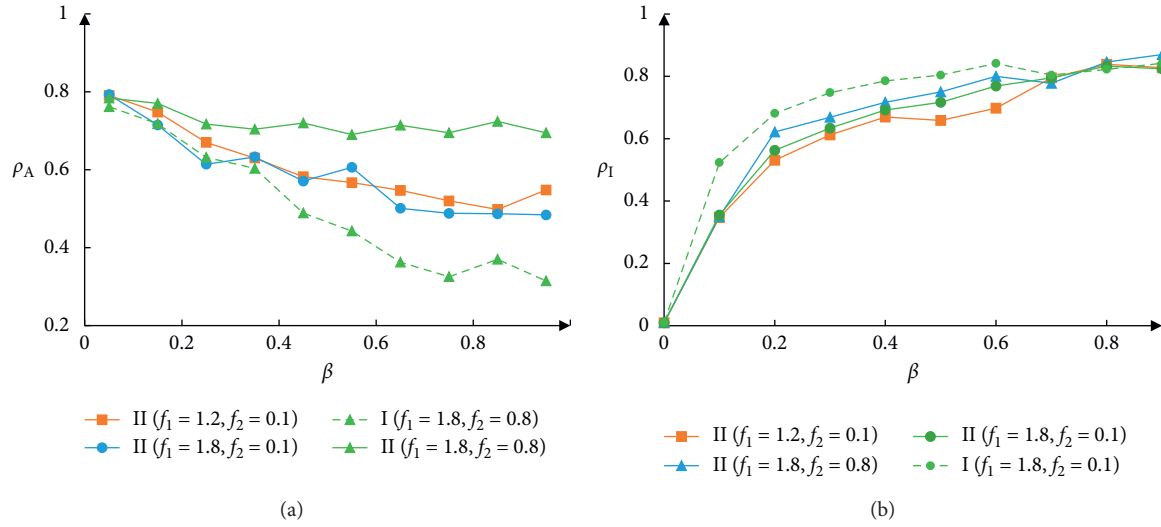


FIGURE 12: The influence of β on ρ_A and ρ_I .

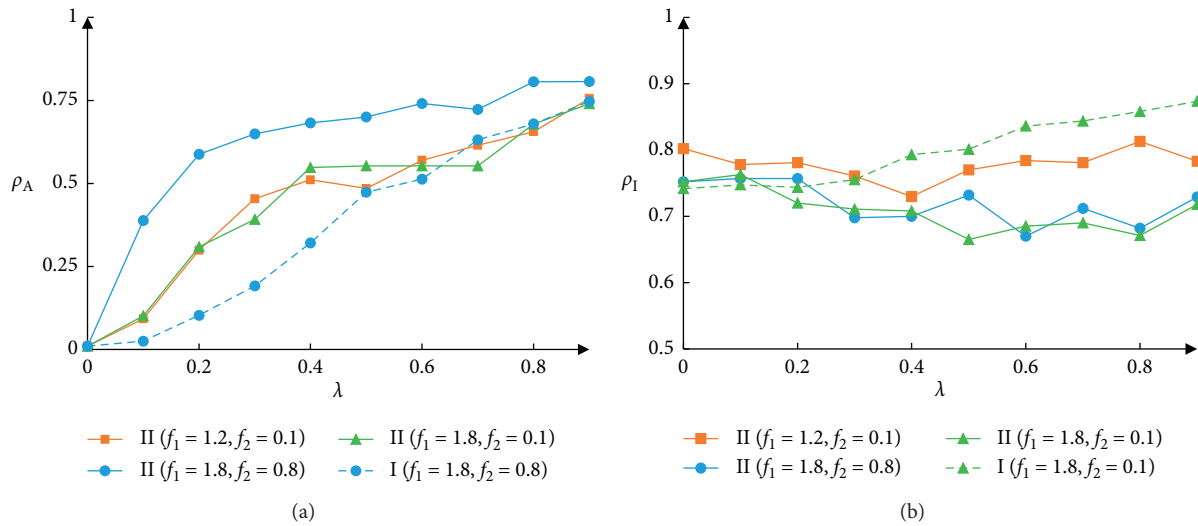


FIGURE 13: The influence of λ on ρ_A and ρ_I .

TABLE 3: Different government control measures and corresponding assumed value of f_1 .

Phase	Date	Government measures	Importance	Assumed value of f_1
1	29 December 2019–22 January 2020	Early detection of the COVID-19 preliminary control	Significant	0.8
2	23 January–29 January 2020	(1) Public health level 1 response of 31 provinces (2) Strict exit screening (3) Medical support from other regions of China (4) Cancellation of mass gatherings (5) Methodological improvement on the diagnosis and treatment strategy	Critical	0.6

TABLE 3: Continued.

Phase	Date	Government measures	Importance	Assumed value of f_1
3	30 January–11 February 2020	(1) Public health level 1 response of 31 provinces (2) Strict exit screening (3) Domestic and international medical support (4) The larger scale of cancellation of mass gatherings (5) Further methodological improvement on the diagnosis and treatment strategy (6) Spontaneous household quarantine by citizens (7) Two newly built hospitals' put into use (8) A clinical trial of perspective medicines	Essential	0.4
4	12 February–20 February 2020	(1) Public health level 1 response of 31 provinces (2) Strict exit screening (3) Further medical support from home and abroad (4) Massive online teaching in a postponed semester (5) Orderly resumption of back to work (6) Addition of new diagnosis method—clinical diagnosis in Hubei Province (7) Interagency mechanism (8) Further exploration of an effective therapeutic strategy	Crucial	0.2

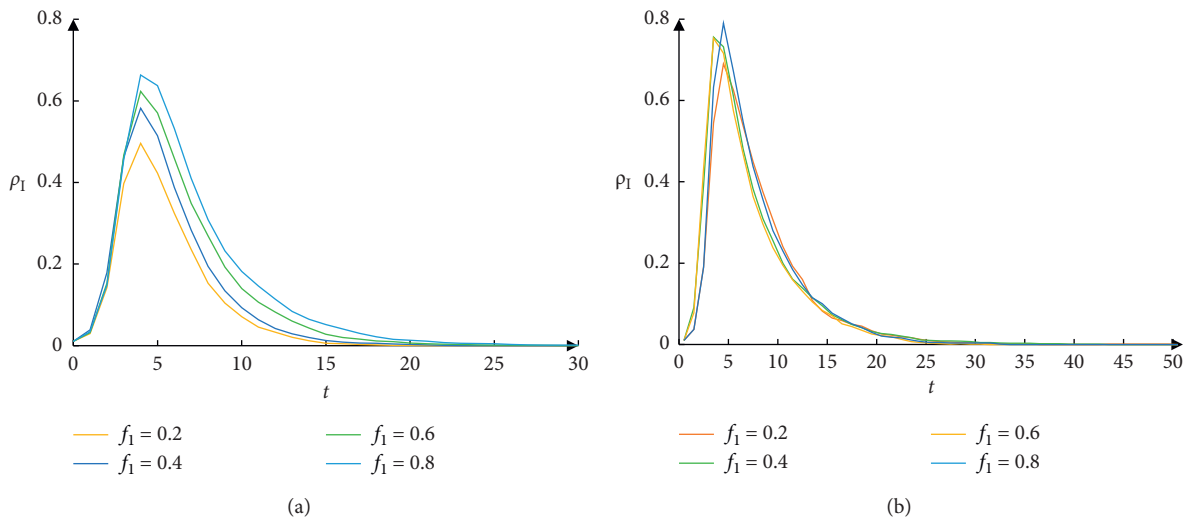


FIGURE 14: Changes in ρ_I under different levels of government measures: (a) Model I; (b) Model II.

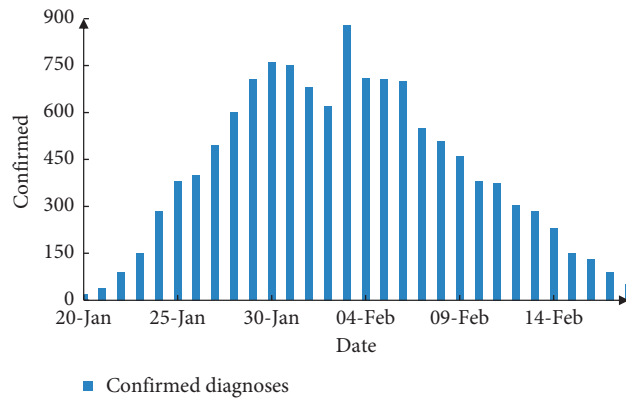


FIGURE 15: The number of newly confirmed diagnoses in regions outside Hubei.

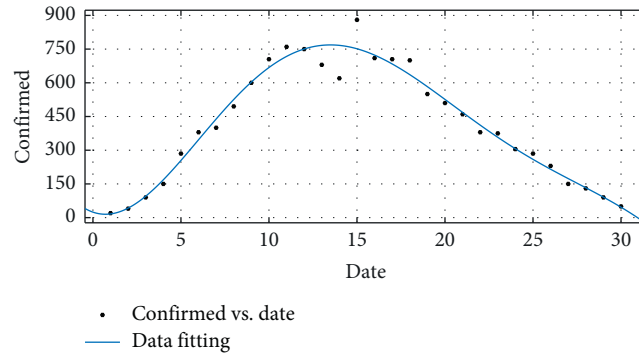


FIGURE 16: Date fitting by ploy regression.

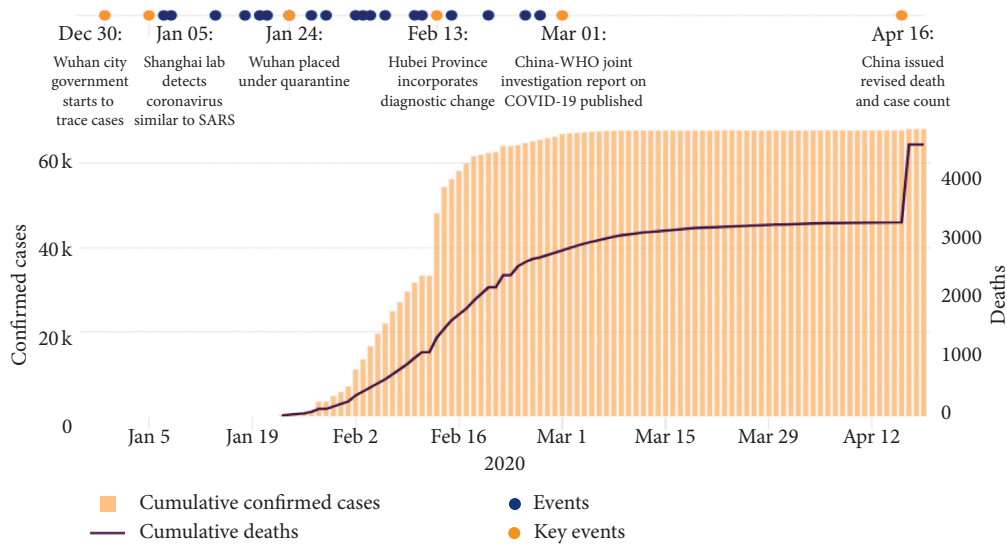


FIGURE 17: Accumulated timetable for confirmed cases in Hubei Province (<https://coronavirus.jhu.edu/map.html>).

TABLE 4: Information report of COVID-19 in Hubei Province and the corresponding assumed value of f_2 .

Phase	Epidemic stage	Information report management changes	Importance	Assumed value of f_2
1	Early period	(1) Holding special meetings (2) Establishment of emergency response teams (3) Issue guidance notice	Significant	1.2
2	Beginning period	(1) CDC has issued guidance documents for many times (2) Video training (3) Answer questions by telephone (4) Issuing guidance notices	Critical	1.5
3	High-risk period	(1) Provide 4 analysis reports of more than 20 pages per day (2) Analyze the characteristics of the disease (3) To assess the trend of the epidemic (4) Provide data support for leaders' decision-making	Crucial	1.8
4	Low-risk period	(1) Timely update of the COVID-19 monitoring analysis report (2) Pay attention to the detailed source and detection route of case information (3) Focus on asymptomatic infected persons and epidemic situation analysis at home and abroad	Essential	1.6

*The information of COVID-19 in the study was mainly obtained from the National Health Commission of the People's Republic of China, Chinese Center for Disease Control and Prevention, WHO, Hubei Provincial for Disease Control and Prevention, and various websites of Chinese government agencies and official media, as well as some previous studies.

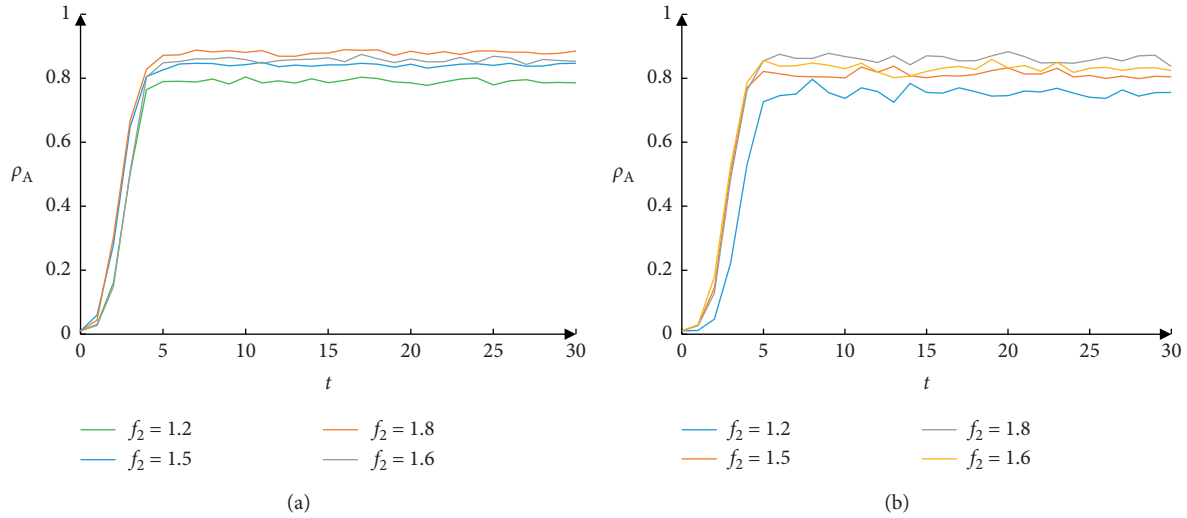


FIGURE 18: Changes in ρ_A under different epidemic stages: (a) Model I; (b) Model II.

data and epidemic prevention process during the spread of COVID-19 can enhance public awareness and effectively control the spread of the epidemic.

6. Conclusions

In this paper, on the one hand, we discuss the interaction between awareness diffusion (including authoritative information and rumors) and epidemic spreading; on the other hand, we analyze the influence of neighbor status on epidemic spreading when awareness diffusion and neighbor behavior are coupled in multiple networks. Distinct from previous studies, people can get epidemic prevention information to reduce the infection rates from their social communication circles, such as microblogs, as well as increase awareness based on their own health status. Moreover, different neighbor status play distinct roles in the awareness acquisition process and the response behavior change process of an individual. We investigate the impact of these factors on epidemic spreading processes and obtain the epidemic threshold with the MMCA approach. Analysis based on the numerical simulations reveal that the epidemic can be reduced by publishing authoritative information to reduce f_1 , publicizing the epidemic prevention process to increase f_2 , and controlling neighbor behavior to be more reasonable, for example, isolating infected neighbors and encouraging them to propagate information related to the epidemic.

Data Availability

The data used to support the findings of this study are available from the corresponding author upon request.

Conflicts of Interest

The authors declare no conflicts of interest.

Acknowledgments

This work was supported by the Education Project of Zhejiang Province (No. Y202045064).

References

- [1] H. A. Rothan and S. N. Byrareddy, "The epidemiology and pathogenesis of coronavirus disease (COVID-19) outbreak," *Journal of Autoimmunity*, vol. 109, Article ID 102433, 2020.
- [2] M. A. Shereen, S. Khan, A. Kazmi, N. Bashir, and R. Siddique, "COVID-19 infection: origin, transmission, and characteristics of human coronaviruses," *Journal of Advanced Research*, vol. 24, pp. 91–98, 2020.
- [3] C.-J. Fan, Y. Jin, L.-A. Huo, C. Liu, Y.-P. Yang, and Y.-Q. Wang, "Effect of individual behavior on the interplay between awareness and disease spreading in multiplex networks," *Physica A: Statistical Mechanics and its Applications*, vol. 461, pp. 523–530, 2016.
- [4] X.-X. Zhan, C. Liu, G. Zhou, Z.-K. Zhang et al., "Coupling dynamics of epidemic spreading and information diffusion on complex networks," *Applied Mathematics and Computation*, vol. 332, pp. 437–448, 2018.
- [5] K. M. A. Kabir, K. Kuga, and J. Tanimoto, "Analysis of SIR epidemic model with information spreading of awareness," *Chaos, Solitons & Fractals*, vol. 119, pp. 118–125, 2019.
- [6] Q. Guo, X. Jiang, and Y. Lei, "Two-stage effects of awareness cascade on epidemic spreading in multiplex networks," *Physical Review E*, vol. 91, no. 1, Article ID 012822, 2015.
- [7] S. Pei, L. Muchnik, and J. S. Andrade Jr., "Searching for super spreaders of information in real-world social media," *Scientific Reports*, vol. 4, p. 5547, 2014.
- [8] S. Funk, E. Gilad, and V. A. A. Jansen, "Endemic disease, awareness, and local behavioural response," *Journal of Theoretical Biology*, vol. 264, no. 2, pp. 501–509, 2010.
- [9] Z. Wang, M. A. Andrews, Z.-X. Wu, L. Wang, and C. T. Bauch, "Coupled disease-behavior dynamics on complex networks: a review," *Physics of Life Reviews*, vol. 15, pp. 1–29, 2015.
- [10] K. M. A. Kabir, K. Kuga, and J. Tanimoto, "Effect of information spreading to suppress the disease contagion on the

- epidemic vaccination game,” *Chaos, Solitons & Fractals*, vol. 119, pp. 180–187, 2019.
- [11] K. A. Kabir, K. Kuga, and J. Tanimoto, “The impact of information spreading on epidemic vaccination game dynamics in a heterogeneous complex network—a theoretical approach,” *Chaos, Solitons & Fractals*, vol. 132, Article ID 109548, 2020.
- [12] C. Granell, S. Gomez, and A. Arenas, “Dynamical interplay between awareness and epidemic spreading in multiplex networks,” *Physical Review Letters*, vol. 111, no. 12, Article ID 128701, 2013.
- [13] S. Funk, E. Gilad, C. Watkins, and V. A. A. Jansen, “The spread of awareness and its impact on epidemic outbreaks,” *Proceedings of the National Academy of Sciences*, vol. 106, no. 16, pp. 6872–6877, 2009.
- [14] W. Wang, Q. H. Liu, and S. M. Cai, “Suppressing disease spreading by using information diffusion on multiplex networks,” *Scientific Reports*, vol. 6, no. 1, pp. 1–14, 2016.
- [15] W. Wang, Q.-H. Liu, J. Liang, Y. Hu, and T. Zhou, “Co-evolution spreading in complex networks,” *Physics Reports*, vol. 820, pp. 1–51, 2019.
- [16] P. Zhu, X. Wang, Q. Zhi, J. Ma, and Y. Guo, “Analysis of epidemic spreading process in multi-communities,” *Chaos, Solitons & Fractals*, vol. 109, pp. 231–237, 2018.
- [17] P. Zhu, X. Wang, S. Li, Y. Guo, and Z. Wang, “Investigation of epidemic spreading process on multiplex networks by incorporating fatal properties,” *Applied Mathematics and Computation*, vol. 359, pp. 512–524, 2019.
- [18] K. M. A. Kabir and J. Tanimoto, “Analysis of epidemic outbreaks in two-layer networks with different structures for information spreading and disease diffusion,” *Communications in Nonlinear Science and Numerical Simulation*, vol. 72, pp. 565–574, 2019.
- [19] L. Y. Shang, “Discrete-time epidemic dynamics with awareness in random networks,” *International Journal of Biomathematics*, vol. 6, no. 2, pp. 147–153, 2013.
- [20] Y. Shang, “Modeling epidemic spread with awareness and heterogeneous transmission rates in networks,” *Journal of Biological Physics*, vol. 39, no. 3, pp. 489–500, 2013.
- [21] F. Bagnoli, P. Lio, and L. Sguanci, “Risk perception in epidemic modeling,” *Physical Review E*, vol. 76, no. 6, Article ID 061904, 2007.
- [22] J. Alstott, P. Panzarasa, and M. Rubinov, “A unifying framework for measuring weighted rich clubs,” *Scientific Reports*, vol. 4, no. 1, pp. 1–6, 2014.
- [23] Q. Wu, X. Fu, and M. Small, “The impact of awareness on epidemic spreading in networks,” *Chaos: an interdisciplinary journal of nonlinear science*, vol. 22, no. 1, Article ID 013101, 2012.
- [24] Z. Wang, C. T. Bauch, S. Bhattacharyya et al., “Statistical physics of vaccination,” *Physics Reports*, vol. 664, pp. 1–113, 2016.
- [25] Z. Li, P. Zhu, and D. Zhao, “Suppression of epidemic spreading process on multiplex networks via active immunization,” *Chaos: An Interdisciplinary Journal of Nonlinear Science*, vol. 29, no. 7, Article ID 073111, 2019.
- [26] J.-Q. Kan and H.-F. Zhang, “Effects of awareness diffusion and self-initiated awareness behavior on epidemic spreading—an approach based on multiplex networks,” *Communications in Nonlinear Science and Numerical Simulation*, vol. 44, pp. 193–203, 2017.
- [27] Q. Guo, Y. Lei, and C. Xia, “The role of node heterogeneity in the coupled spreading of epidemics and awareness,” *PLoS One*, vol. 11, no. 8, Article ID e0161037, 2016.
- [28] P. Zhu, Q. Zhi, Y. Guo, and Z. Wang, “Analysis of epidemic spreading process in adaptive networks,” *IEEE Transactions on Circuits and Systems II: Express Briefs*, vol. 66, no. 7, pp. 1252–1256, 2018.
- [29] X. Chen, K. Gong, R. Wang, S. Cai, and W. Wang, “Effects of heterogeneous self-protection awareness on resource-epidemic coevolution dynamics,” *Applied Mathematics and Computation*, vol. 385, Article ID 125428, 2020.
- [30] Y. Pan and Z. Yan, “The impact of individual heterogeneity on the coupled awareness-epidemic dynamics in multiplex networks,” *Chaos: An Interdisciplinary Journal of Nonlinear Science*, vol. 28, no. 6, Article ID 063123, 2018.
- [31] M. C. M. Balemans, M. M. H. Huibers, N. W. D. Eikelenboom et al., “Reduced exploration, increased anxiety, and altered social behavior: autistic-like features of euchromatin histone methyltransferase 1 heterozygous knockout mice,” *Behavioural Brain Research*, vol. 208, no. 1, pp. 47–55, 2010.
- [32] H. Faneca, V. A. Figueiredo, I. Tomaz et al., “Vanadium compounds as therapeutic agents: some chemical and biochemical studies,” *Journal of Inorganic Biochemistry*, vol. 103, no. 4, pp. 601–608, 2009.
- [33] K. Hukushima and K. Nemoto, “Exchange Monte Carlo method and application to spin glass simulations,” *Journal of the Physical Society of Japan*, vol. 65, no. 6, pp. 1604–1608, 1996.
- [34] A. P. Lyubartsev, A. A. Martsinovski, S. V. Shevkunov, and P. N. Vorontsov-Velyaminov, “New approach to Monte Carlo calculation of the free energy: method of expanded ensembles,” *The Journal of Chemical Physics*, vol. 96, no. 3, pp. 1776–1783, 1992.
- [35] Y. Fang, Y. Nie, and M. Penny, “Transmission dynamics of the COVID-19 outbreak and effectiveness of government interventions: a data-driven analysis,” *Journal of Medical Virology*, vol. 92, no. 6, pp. 645–659, 2020.
- [36] Y. C. Chen, P. E. Lu, and C. S. Chang, “A time-dependent SIR model for COVID-19 with undetectable infected persons,” *IEEE Transactions on Network Science and Engineering*, vol. 7, no. 4, pp. 3279–3294, 2020.